LA-UR- 08-8044

Approved for public release; distribution is unlimited.

Title:	Neutron inelastic scattering in natural Pb as a background in neutrinoless double-beta decay experiments
Author(s):	V.E. Guiseppe S.R. Elliott A. Hime D.V. Perepelitsa
Intended for:	Posting on arXiv and submission to Physical Review C

Form 836 (7/06)

Neutron inelastic scattering in natural Pb as a background in neutrinoless double-beta decay experiments

V.E. Guiseppe,* S.R. Elliott, A. Hime, and D.V. Perepelitsa
Physics Division, Los Alamos National Laboratory, Los Alamos, NM 87545

M. Devlin, N. Fotiades, and R.O. Nelson
LANSCE Division, Los Alamos National Laboratory, Los Alamos, NM 87545

D.-M. Mei
Department of Earth Science and Physics, University of South Dakota, Vermillion, South Dakota 57069
(Dated: July 29, 2008)

Inelastic neutron scattering on Pb isotopes can result in γ rays near the signature endpoint energy in a number of $\beta\beta$ isotopes. In particular, there are γ-ray transitions in ^{206}Pb and ^{207}Pb that might produce energy deposits at the ^{76}Ge $Q_{\beta\beta}$ in Ge detectors used for $0\nu\beta\beta$ searches. The levels that produce these γ rays can be excited by n,n$'\gamma$ reactions, but the cross sections are small and previously unmeasured. The cross section on $^{\rm nat}$Pb to produce the 2041-keV γ ray from ^{206}Pb is measured to be 3.1 $\pm$ 0.6 (stat.) $\pm$ 0.3 (syst.) mb at $\approx$ 9.6 MeV. The cross section on $^{\rm nat}$Pb to produce the 3062-keV γ ray from ^{207}Pb is measured to be 4.3 $\pm$ 0.8 (stat.) $\pm$ 0.4 (syst.) mb at the same energy. We place upper limits on the cross sections for exciting some other levels in Pb that have transition energies corresponding to $Q_{\beta\beta}$ in other $\beta\beta$ isotopes.

PACS numbers: 23.40.-s, 25.40.Fq

I. INTRODUCTION

Neutrinoless double-beta decay ($0\nu\beta\beta$) plays a key role in understanding the neutrino's absolute mass scale and particle-antiparticle nature [1–6]. If this nuclear decay process exists, one would observe a mono-energetic line originating from a material containing an isotope subject to this decay mode. One such isotope that may undergo this decay is ^{76}Ge. Germanium-diode detectors fabricated from material enriched in ^{76}Ge have established the best half-life limits and the most restrictive constraints on the effective Majorana mass for the neutrino [7, 8]. One analysis [9] of the data in Ref. [8] claims evidence for the decay with a half-life of $2.23^{+0.44}_{-0.31}\times10^{25}$ y. Planned Ge-based $0\nu\beta\beta$ experiments [10, 11] will test this claim. Eventually, these future experiments target a sensitivity of $>10^{27}$ y or $\sim$1 event/ton-year to explore neutrino mass values near that indicated by the atmospheric neutrino oscillation results.

The key to these experiments lies in the ability to reduce intrinsic radioactive background to unprecedented levels and to adequately shield the detectors from external sources of radioactivity. Previous experiments' limiting backgrounds have been trace levels of natural decay chain isotopes within the detector and shielding components. The γ-ray emissions from these isotopes can deposit energy in the Ge detectors producing a continuum, which may overwhelm the potential $0\nu\beta\beta$ signal peak at 2039 keV. Great progress has been made identifying the location and origin of this contamination, and future efforts will substantially reduce this contribution to the background. The background level goal of 1 event/ton-year, however, is an ambitious factor of $\sim$400 improvement over the currently best achieved background level [8]. If the efforts to reduce the natural decay chain isotopes are successful, previously unimportant components of the background must be understood and eliminated. The work of Mei and Hime[12] recognized that $(n, n'\gamma)$ reactions will become important for ton-scale double-beta decay experiments.

Reference [13] recognized that the specific γ rays from Pb isotopes at 2041 and 3062 keV are particularly troublesome. The former is dangerously near the 2039.00$\pm$0.05-keV Q-value for zero-neutrino double-beta decay in ^{76}Ge and the latter can produce a double-escape peak line at 2040 keV. That paper pointed out that the cross sections to produce these lines in $^{\rm nat}$Pb were unmeasured and hence set to zero in the data bases of the simulation codes used to design and analyze $0\nu\beta\beta$ data. The paper also attempted an initial estimate of the cross section, but made it clear that better measurements were required.

Previous authors have studied n,n$'\gamma$ reactions in Pb usually using enriched samples to isolate the isotopic effects[14, 15]. However, only [13] has attempted to report results for the small-cross-section transitions that produce the lines of interest for ^{76}Ge $0\nu\beta\beta$. This paper presents measurements of Pb(n,n$'\gamma$) production cross section of the γ rays at 2041 and 3062 keV for $^{\rm nat}$Pb. These γ rays are produced by the relaxation of the 3744 keV level in ^{206}Pb and the 3633 level in ^{207}Pb respectively. Although our work was motivated by neutron reaction

*guiseppe@lanl.gov

considerations in materials that play important roles in the MAJORANA [16] design, the results have wider utility since lead is used by numerous low-background experiments.

II. EXPERIMENT

Data were collected at the Los Alamos Neutron Science Center (LANSCE) Weapons Neutron Research (WNR) facility [17]. As the broad-spectrum, pulsed neutron beam strikes the Pb target, the outgoing γ rays are detected by the GEANIE spectrometer [18]. GEANIE is located a distance of 20.34 m from the natural tungsten spallation target.

The primary target used was a 2.5-mm thick natural Pb (^{nat}Pb) foil angled 20° off the normal of the beam direction. The GEANIE spectrometer consists of 26 HPGe detectors; 20 of which have BGO active shields. Of the 26 Ge detectors, 16 are coaxial geometry with a dynamic range up to 4 MeV and 10 are planar geometry detectors with a limited dynamic range of 1 MeV. Due to the high γ-ray energy region of interest for $0\nu\beta\beta$, only the coaxial detectors were considered here. Many of the GEANIE coaxial detectors had reduced resolution, due either to neutron damage or other issues, and only the four detectors with the best energy and timing resolution were used in this analysis.

Some of the detectors have Pb collimators surrounding their face to select mainly radially-directional γ rays from the target. A majority of the data collected occured with the detectors in this configuration. This may present additional Pb for neutron interaction, but since this Pb was not in the path of the neutron beam, it is assumed that this contribution is negligible and therefore not considered in our analysis.

The pulsed neutron beam has the following timing structure. Macropulses, lasting 625 μs, occur at a rate of 40 Hz. Micropulses are spaced every 1.8 μs, during which the neutron energy is determined by the time of flight from the micropulse start. An in-beam fission chamber measures the neutron flux with ^{235}U and ^{238}U foils. In addition to the ^{nat}Pb data, there were source runs for calibration purposes. Data were collected from two radioactive sources, ^{152}Eu and ^{226}Ra, with the neutron beam shuttered. Analysis of the sources permit a relative efficiency curve for the detector array.

III. ANALYSIS AND RESULTS

A. Analysis description

The data collected from GEANIE are stored in an event mode file containing time and pulse-height information from each HPGe detector and the fission chamber. Data from each detector must be checked for integrity and aligned to adequately sum together with the others. The analysis permits gating the resulting Ge-detector energy spectra on neutron energy to achieve a neutron energy dependence on the γ-ray production.

The absolute efficiency of each detector was determined by constructing an efficiency curve based on the two sources counted. Using 22 lines in Eu and 29 in Ra, the known source activities and branching ratios, and the approximate run live time, an efficiency curve was generated from a fit to the calculated efficiencies. The run time is not known exactly but estimated using scaler counts from a pulser. The scale of the absolute efficiency is corrected by the normalization discussed in Section III B. A correction is needed for attenuation of γ-rays in the target. Based on the location of the four working detectors, a path length seen by each detector through the Pb target is determined. An energy-dependent attenuation correction is calculated by integrating the exponential attenuation expression over the total path length through the Pb target. This correction is combined with the detector efficiency determined from the source data to obtain an efficiency correcting for target attenuation. The net corrected efficiency for the array is the sum of the detector's corrected efficiencies. No correction was made for multiply scattered neutrons in the target due to the low probability of successive reactions involving the rare γ-rays of interest.

B. Cross Sections

With an array like GEANIE, observation of the angular dependance of the γ rays is possible. However, with only four detectors used at four unique angles, this technique is not optimal. Instead, an integral γ-ray production cross section is calculated based on the net γ-ray yield of the array.

Each γ-ray event detected has timing information, which can be referenced to the start of a pulse for time-of-flight neutron energy determination. The γ-ray spectrum is gated into a number of individual spectra corresponding to a fixed time interval but increasing neutron-energy width. The γ-ray lines of interest are fitted via the RADWARE package [19] to obtain γ-ray yields as a function of neutron energy.

The flux measured by the fission chamber is gated into the same neutron bins using the same γ flash and time-of-flight technique, but corrected to determine the neutron energy at the target location and not the fission chamber location. The resulting gated fission chamber pulse height spectra is analyzed using the known neutron-induced fission cross sections of ^{238}U to determine neutron flux.

The angle-integrated γ-ray cross section ($\sigma_\gamma(E_n)$) can be calculated using

$$\sigma_\gamma(E_n) = \frac{I_\gamma}{T_\gamma\,\epsilon_\gamma}\frac{T_\Phi}{\Phi}\frac{1+\alpha}{t}N \qquad (1)$$

where I_γ is the γ-ray yield [counts/MeV], Φ is the neu-

tron yield [neutron/MeV], ϵ_γ is the absolute γ-ray detection efficiency, t is the target aerial density [atoms/barn], α is the internal conversion coefficient, T_γ and T_Φ are the fractional live times of the HPGe detectors and fission chamber, respectively, and N is a normalization factor based on a known cross section.

If the normalization factor is calculated from the same data set, the energy-independent factors cancel, so

$$\sigma_\gamma(E_n) = \frac{I_\gamma}{\epsilon_\gamma}\frac{1+\alpha}{\Phi}N^{eff} \quad (2)$$

An effective normalization factor, N^{eff}, is defined as

$$N^{eff} = \sigma_K \frac{\epsilon_\gamma^K}{I_\gamma^K}\frac{\Phi^K}{1+\alpha^K} \quad (3)$$

where σ_K is a known cross section in ^{nat}Pb corresponding to a given transition labeled K. Neglecting the energy-independent contributions to the cross section allows a reduction in the uncertainty budget.

The prominent lines in the major Pb isotopes have been studied in detail [14, 15] and serve as a convenient reference and known transition for normalization. The recent study [14] of Pb isotopes showed good agreement between past experimental results and that of the TALYS [20] nuclear reaction code. The TALYS code ran with primarily default settings with proper treatment of long-lived isomers. The pulsed structure of the LANSCE beam and the time-of-flight gating allows the detection of prompt decays while long-lived isomers are a background.

Three of the strongest lines in ^{nat}Pb are analyzed and compared against the TALYS result for normalization. The three transitions are the $3^- \rightarrow 0^+$ 2614.5-keV γ ray in ^{208}Pb, the $\frac{5}{2}^- \rightarrow \frac{1}{2}^-$ 569.7-keV γ ray from ^{207}Pb, and the $2^+ \rightarrow 0^+$ 803.1-keV γ ray from ^{206}Pb. These three major lines were analyzed using 15 ns time-of-flight neutron binning, which is the resolution limit of the HPGe detectors. Gamma-ray production cross sections are calculated using TALYS to represent the production in ^{nat}Pb by summing and weighting by isotopic abundance. Therefore the 803-keV γ ray can be produced through the following reaction channels: ^{206}Pb(n,n'γ)^{206}Pb, ^{207}Pb(n,2nγ)^{206}Pb, and ^{208}Pb(n,3nγ)^{206}Pb. Similarly, the 570-keV γ ray can be produced through the two channels: ^{207}Pb(n,n'γ)^{207}Pb and ^{208}Pb(n,2nγ)^{207}Pb. The 2615-keV γ ray only results from ^{208}Pb(n,n'γ)^{208}Pb. To obtain the normalization factor, the output of TALYS and experimental results were compared over the dominant neutron range of 4-7 MeV where the production rates for these lines are strongest. A normalization factor resulting from this analysis is estimated to be 1.22 ± 0.04 (0.3%).

The two lines of most interest to Ge-based $0\nu\beta\beta$ experiments using Pb shielding are weak and were observable in these data only by summing spectra over a large range of neutron energies. The 2040-keV γ ray is most dominant in the 4-30 MeV neutron range while the 3062-keV

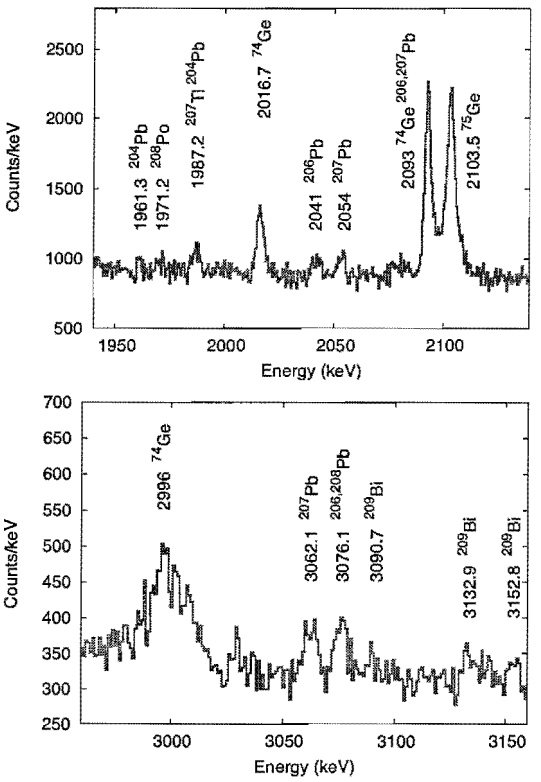

FIG. 1: The γ-ray spectra showing the 2041-keV γ-ray line and the 3062-keV γ-ray line (6.7-12.5 MeV neutrons).

γ ray is most dominant in the range from 4-13 MeV neutron range (Fig. 1). For cross section analysis, the γ-ray spectra were gated by a larger bin width of 150 ns, which resulted in 9 bins covering the energy range of 1-200 MeV. For those bins where a peak was not observed, a sensitivity limit was measured to provide an upper limit on the cross section. The internal conversion coefficients for these two transitions are not known and are assumed to be zero.

Applying the normalization, the cross sections for the 2041 and 3062-keV γ-ray lines are obtained (Figs. 2 and 3). The results are 3-5 mb for both the 2041 and 3062-keV lines for neutron energies near 10 MeV. The experimental results are higher than that predicted by a TALYS calculation for these γ-ray transitions.

C. Measurement Uncertainty

The systematic and statistical uncertainties encountered are listed in Table I. The normalization correction uncertainty is estimated from the agreement of normalization factors obtained from the three prominent lines compared against known cross sections. The three known transitions have an experimental uncertainty of less than

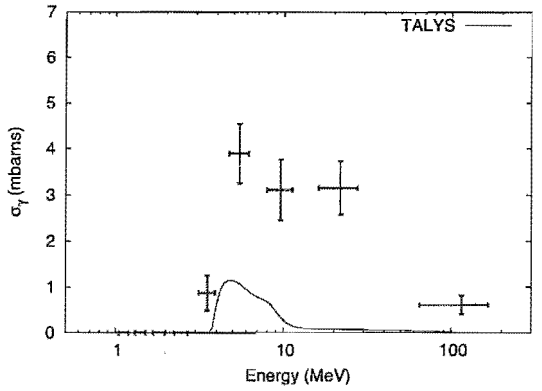

FIG. 2: The observed γ-ray production cross section for the 2041-keV γ ray in ^{206}Pb.

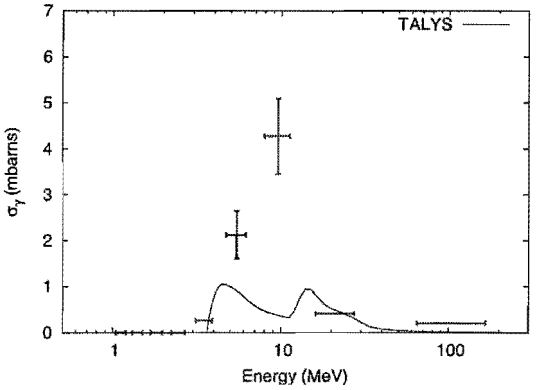

FIG. 3: The observed γ-ray production cross section for the 3062-keV γ ray in ^{207}Pb.

$\sim$7% in the energy range 3-10 MeV and so we include a 7% systematic uncertainty. The efficiency curve uncertainty derives from the error in the fit to the the source data and the error in the attenuation correction, which is dominated by the uncertainty in the parameterized mass attenuation coefficient [21] and the tolerance of the target thickness. The statistical errors in the flux and yield measurements are based on the counts in the fission chamber and γ-ray detectors, respectively. The uncertainty of the neutron energy is based on the timing resolution of the HPGe detectors. The statistics of the weak lines of interest are the dominant source of uncertainty.

Generally, the angle-integrated γ-ray cross section is computed from an integral of the differential cross section. The γ-ray differential cross section can be expanded in a sum of Legendre polynomials and, excluding contribution from cascades, can be predicted for transition between some states [22] near threshold. Higher energies and contributions from cascades diminish anisotropy in the angular distribution. In this experiment, the γ-ray yield was the sum of the yields of four detectors and assumes an isotropic distribution. Ref. [14, 22] define anisotropic distributions for the E2, E3, and M1+E2 multipolarities. Those distribution show no more than a 6% deviation from isotropic assumption when evaluated at the locations of the four detectors used ($\cos\theta = 0.1818$, 0.2267, 0.5492, 0.8745). Further, Reference [23] tabulates angular distribution corrections when assuming an isotropic distribution and finds correction mainly within 5%. We include a 6% systematic uncertainty to account for any γ-ray angular distribution.

TABLE I: A listing of the systematic and statistical uncertainties in the cross section measurement.

	Systematic Uncertainty	
	2040-keV γ ray	3062-keV γ ray
normalization	0.35%	0.35%
efficiency	1.22%	1.25%
angular correction	6%	6%
known transitions	7%	7%

	Statistical Uncertainty		
neutron energy (MeV)	neutron flux	2040-keV γ-ray yield	3062-keV γ-ray yield
1.00-1.24	5.1%		
1.24-1.58	2.2%		
1.58-2.08	1.0%		
2.08-2.87	0.92%		
2.87-4.20	0.87%	44%	
4.20-6.72	0.76%	15%	24%
6.72-12.50	0.62%	20%	18%
12.50-31.15	0.60%	17%	
31.15-200	0.49%	33%	

IV. DISCUSSION AND CONCLUSION

The cross sections of interest to Ge $0\nu\beta\beta$ are tabulated in Table II. In Ref. [13] an estimate for the cross section of the ^{207}Pb(n,n' 3062-keV γ ray)^{207}Pb was given as 75 mb with an uncertainty of about 20%. For ^{nat}Pb this would indicate a cross section for comparison of $\approx$16 mb at an average neutron energy of $\approx$4.5 MeV. Considering the caveats discussed in the previous work with regards to the presence of Cl, that this cross section is a factor of a few above the values reported in this work is considered to be consistent. Reference [13] did not provide a value for the cross section for the production of the 2041 γ ray.

Table III lists a number of frequently used isotopes for $\beta\beta$ and their Q values. In addition the table lists Pb isotopes which have transitions near 3 critical energies for each isotope. A γ ray with an energy similar to that of the Q value can produce a background line that might mimic $0\nu\beta\beta$ in an experiment that uses a Pb as a shield or for some other apparatus component. In addition, however, γ rays that pair produce in a detector but have either one (single escape peak) or both (double escape peak) annihilation γ rays escape the detector may also produce a line feature at the $0\nu\beta\beta$ endpoint for a give initial γ-ray

TABLE II: The summary of the cross sections as a function of energy for the 2041 and 3062-keV transitions.

neutron energy (MeV)	Cross section (mb) $^{nat}Pb(n,xn\gamma)^{206}Pb$ 2041 keV	$^{nat}Pb(n,xn\gamma)^{207}Pb$ 3062 keV
2.87-4.20	0.87 ± 0.38(stat.) ± 0.08 (syst.)	<0.3
4.20-6.72	3.9 ± 0.6 (stat.) ± 0.4 (syst.)	2.1 ± 0.5 (stat.) ± 0.2(syst.)
6.72-12.50	3.1 ± 0.6 (stat.) ± 0.3 (syst.)	4.3 ± 0.8 (stat.) ± 0.4 (syst.)
12.50-31.15	3.2 ± 0.5 (stat.) ± 0.3 (syst.)	<0.4
31.15-200	0.61 ± 0.20 (stat.) ± 0.06 (syst.)	<0.2

energy. Such γ rays would be 511 keV and 1022 keV more energetic than the Q value. Also in Table III, we provide cross sections or upper limits on the cross sections to excite the levels that produce these γ rays in ^{nat}Pb.

We have measured the cross sections for the production of γ rays of interest to Pb-shielded Ge $0\nu\beta\beta$ experiments relative to previously measured strong transistions and the results are presented in Table II. The cross sections are small (few mb) near 5-10 MeV and are below our sensitivity by about 40 MeV. The cross sections can be folded with the underground neutron flux to estimate background rates for such experiments. Although, the rates will likely be very low, the overall background must be extremely low to have the required sensitivity to $0\nu\beta\beta$.

Acknowledgments

This work was supported in part by Laboratory Directed Research and Development at Los Alamos National Laboratory. This work benefited from the use of the Los Alamos Neutron Science Center, funded by the U.S. Department of Energy under contract DE-AC52-06NA25396.

[1] S. R. Elliott and P. Vogel, Ann. Rev. Nucl. Part. Sci. **52**, 115 (2002).
[2] S. R. Elliott and J. Engel, J. Phys. G: Nucl. Part. Phys. **30**, R 183 (2004).
[3] A. S. Barabash, F. Hubert, P. Huber, , and V. I. Umatov, Pisma v ZhETF **79**, 12 (2004).
[4] F. T. III. Avignone, G. S. K. III, and Y. Zdesenko, New Journal of Physics **7**, 6 (2005).
[5] H. Ejiri, J. Phys. Soc. Jap. **74**, 2101 (2005).
[6] F. T. III. Avignone, S. Elliott, and J. Engel, Rev. Mod. Phys. **80**, 481 (2008), arXiv:0708.1033.
[7] C. E. Aalseth et al. (IGEX), Phys. Rev. D. **65**, 092007 (2002).
[8] L. Baudis et al., Phys. Rev. Lett. **83**, 41 (1999).
[9] H. V. Klapdor-Kleingrothaus and I. V. Krivosheina, Mod. Phys. Lett. A **21**, 1547 (2006).
[10] The Gerda Collaboration (2004), hep-ex/0404039.
[11] S. R. Elliott (2008), arXiv:0807.1741 [nucl-ex].
[12] D.-M. Mei and A. Hime, Phys. Rev. D **73**, 053004 (2006), astro-ph/0512125.
[13] D.-M. Mei, S. R. Elliott, V. M. Gehman, A. Hime, and K. Kazkaz (2008), in press, nucl-ex/0704.0306v2.
[14] L.-C. Mihailescu, Ph.D. thesis, University of Bucharest (2006).
[15] H. Vonach, A. Pavlik, M. B. Chadwick, R. C.Haight, R. O. Nelson, S. A. Wender, and P. G. Young, Phys. Rev. C **50**, 1952 (1994).
[16] F. T. Avignone III (2007), arXiv:0711.4808v1 [nucl-ex].
[17] P. W. Lisowski, C. D. Bowman, G. J. Russell, and S. A. Wender, Nucl. Sci. Eng. **106**, 208 (1990).
[18] J. A. Becker and R. O. Nelson, Nucl. Phys. News Int. **7**, 11 (June, 1997).
[19] URL `http://radware.phy.ornl.gov/`.
[20] A. J. Koning, S. Hilaire, and M. C. Duijvestijn, in *Proceedings of the International Conference on Nuclear Data for Science and Technology - ND2004*, edited by R. C. Haight, M. B. Chadwick, T. Kawano, and P. Talou (AIP vol. 769, Sep. 26 - Oct. 1, 2004, Santa Fe, USA, 2005), p. 1154.
[21] V. I. Gudima and G. V. Pekina, Atomnaya Energiya **48** (1980).
[22] E. Sheldon and D. M. Van Patter, Rev. Mod. Phys. **38**, 143 (1966).
[23] N. Fotiades et al. (2001), LA-UR-01-4281.
[24] G. Audi, A. H. Wapstra, and C. Thibault, Nucl. Phys. A **729**, 337 (2003).
[25] S. Rahaman et al. (2007), arXiv:0712.3337.
[26] M. Redshaw et al., Phys. Rev. Lett. **98**, 053003 (2007).

TABLE III: A list of frequently studied isotopes for $\beta\beta$ and their Q values[24–26]. In columns 3-5 are indicated Pb isotopes with levels that emit γ rays near the energies of the Q value, the Q value + 511 keV (SEP, Single Escape Peak), and the Q value + 1022 keV (DEP, Double Escape Peak) respectively. Also in columns 3-5 are the cross section values or upper limits for exciting the transitions in ^{nat}Pb with neutrons of energy 6.72-12.50 MeV. Where the cross section is listed as NA, we were unable to place a limit due to the γ-ray energy being outside the range of the detection system. The line arguably present at the SEP for ^{116}Cd would be due to a transition we are unable to identify.

$\beta\beta$ Isotope	$Q_{\beta\beta}$ (keV)	γ ray	SEP	DEP
^{76}Ge	2039.00 ± 0.05	^{206}Pb $\sigma = 3.1 \pm 0.7$ mb		^{207,208}Pb $\sigma = 4.3 \pm 0.8$ mb
^{82}Se	2995.5 ± 1.9			^{208}Pb σ NA
^{100}Mo	3034.40 ± 0.17	^{208}Pb $\sigma < 0.4$ mb	^{206}Pb $\sigma = 2.6 \pm 0.5$ mb	^{206}Pb σ NA
^{116}Cd	2809 ± 4		$\sigma = 0.67 \pm 0.47$ mb	
^{130}Te	2530.3 ± 2.0		^{208}Pb $\sigma < 0.4$ mb	
^{136}Xe	2457.83 ± 0.37	^{206,208}Pb $\sigma < 0.3$ mb		
^{150}Nd	3367.7 ± 2.2			^{207}Pb σ NA